

Electronic Supplementary Information

Selective separation of larger molecules from Lewis base mixture by flexible one-dimensional Cu(II) coordination polymer with shape-recognizing space

Shin-ichiro Noro,* Tomoyuki Akutagawa, and Takayoshi Nakamura*

Research Institute for Electronic Science, Hokkaido University, Sapporo 001-0020, Japan

Fax: +81-11-706-9420; Tel: +81-11-706-9418

E-mail: noro@es.hokudai.ac.jp & tnaka@es.hokudai.ac.jp

Experimental Section

General. $[\text{Cu}(\text{PF}_6)_2(\text{bpetha})_2]_n$ (**1**) was prepared according to the literature.¹ ¹H-NMR spectra in acetone-d6 were measured by JEOL ECX-600 and 400 NMR spectrometers. UV-vis reflection spectra were recorded using a Hitachi U-3500 spectrophotometer with a resolution of 0.5 nm. Thermogravimetric analyses were performed using a Rigaku Thermo Plus TG8120 apparatus in the temperature range between 298 and 773 K in a N₂ atmosphere and at a heating rate of 10 K min⁻¹. XRD data of powder samples were collected on a Rigaku RINT-Ultima III diffractometer with CuK α radiation. The adsorption isotherms at 298 K were measured with BELSORP volumetric adsorption equipment (BELSORP-max for H₂O, MeOH, and THF, BELSORP-18 for MeCN, and BELSORP-aqua for EtOH and 2-butanone).

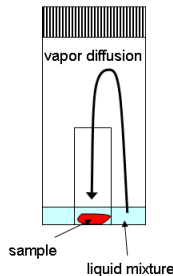
Synthesis of $\{\text{[Cu(4-phenylpyridine)}_4(\text{acetone})_2]\cdot\text{2PF}_6\}$ (2**–2acetone).** A MeCN solution (40 mL) of 4-phenylpyridine (1.55 g, 10 mmol) was added to an H₂O solution (50 mL) containing Cu(BF₄)₂·6H₂O (0.863 g, 2.5 mmol) and KPF₆ (1.84 g, 10 mmol). The obtained blue suspension was stirred on a hot plate until MeCN was completely removed. The obtained blue microcrystals were filtered, washed with H₂O, and dried in vacuum at 343 K overnight. The recrystallization from acetone/hexane gave single crystals of **2**–2acetone.

X-ray Structural Analysis. X-ray diffraction measurement on **2**–2acetone was performed using a Rigaku RAXIS-RAPID imaging plate diffractometer using graphite-monochromated Mo K α radiation ($\lambda = 0.71073 \text{ \AA}$). The data were corrected for Lorentz and polarization effects. The structure was solved using direct methods (SIR2002)² and expanded using Fourier techniques.³ All nonhydrogen atoms were refined anisotropically. All the hydrogen atoms were refined using the riding model. The refinements were carried out using full-matrix least-squares techniques on F^2 . All calculations were performed using the CrystalStructure crystallographic software package.⁴ The crystal data are summarized in Tables S1 and S2. The crystal structure around the Cu(II) center is shown in Fig. S6. The crystallographic data in CIF format are available from the Cambridge Crystallographic Data Centre, CCDC reference number 734111.

Calculation of potential energy. Atomic coordinates based on the X-ray crystal structure analysis of $\{\text{[Cu(4-phenylpyridine)}_4(\text{acetone})_2]\cdot\text{2PF}_6\}$ (**2**) were used for the calculation for the acetone guest. The 4-positions of the pyridine rings were replaced by H, and one acetone molecule was removed, to simplify the structure. For the MeCN, 2-butanone, and THF guests, each guest was located at the optimal axial position of the Cu(II) ion. The relative energy of the $[\text{Cu}(\text{pyridine})_4(\text{G})]$ (G = MeCN, acetone, 2-butanone, and THF) model structure (as shown in Fig. S7) was calculated by using the UHF/6-31(d) basis set.⁵ The axial Cu-O(N) distances were moved at 0.1 Å intervals, and the relative energies were calculated by using fixed atomic coordinates.

Detailed experimental procedure for investigating separation properties. A 10 mg of the desolvated **1** was set in a smaller sample tube (1.8 mL volume). The smaller tube was set inside a larger tube (20 mL volume) with 0.4 mL of liquid mixture as shown in the figure below, in which the sample does not have contact with liquid mixture. After capped, the larger tube was allowed to stand for 1 hour at room temperature. The formation of the 2-

butanone adducts was confirmed by XRD and TG measurements (Fig. S8 and S9). The smaller tube was picked up from the larger tube and allowed to stand for 10 minutes at room temperature. Then, a 1 mL of acetone-d⁶ was added to the smaller tube to extract the adsorbed guests. The complete exchange of axial guests was confirmed by XRD and TG measurements (Fig. S10-S12). After 30 minutes, the solution was centrifugalized for 10 minutes and the supernatant solution was used for measurements of ¹H-NMR spectra. A typical ¹H-NMR chart is shown in Fig. S13.



References

- 1 S. Noro, S. Horike, D. Tanaka, S. Kitagawa, T. Akutagawa, T. Nakamura, *Inorg. Chem.*, 2006, **45**, 9290.
- 2 SIR2002, M. C. Burla, M. Camalli, B. Carrozzini, G. L. Cascarano, C. Giacovazzo, G. Polidori, R. Sapgna, *J. Appl. Crystallogr.*, 2003, **36**, 1103.
- 3 DIRDIF-94, P. T. Beurskens, G. Admiraal, G. Beurskens, W. P. Bosman, R. de Gelder, R. Israel, J. M. M. Smits, *The DIRDIF-94 program system, Technical Report of the Crystallography Laboratory*; University of Nijmegen: The Netherlands, 1994.
- 4 *Crystal Structure Analysis Package*, Crystal Structure 3.7.0; Rigaku and Rigaku/MSC: The Woodlands, TX, 2000-2005.
- 5 M. J. Frisch, G. W. Trucks, H. B. Schlegel, G. E. Scuseria, M. A. Robb, J. R. Cheeseman, J. A. Montgomery, Jr., T. Vreven, K. N. Kudin, J. C. Burant, J. M. Millam, S. S. Iyengar, J. Tomasi, V. Barone, B. Mennucci, M. Cossi, G. Scalmani, N. Rega, G. A. Petersson, H. Nakatsuji, M. Hada, M. Ehara, K. Toyota, R. Fukuda, J. Hasegawa, M. Ishida, T. Nakajima, Y. Honda, O. Kitao, H. Nakai, M. Klene, X. Li, J. E. Knox, H. P. Hratchian, J. B. Cross, V. Vakken, C. Adamo, J. Jaramillo, R. Gomperts, R. E. Stratmann, O. Yazyev, A. J. Austin, R. Cammi, C. Pomelli, J. W. Ochterski, P. Y. Ayala, K. Morokuma, G. A. Voth, P. Salvador, J. J. Dannenberg, V. G. Zakrzewski, S. Dapprich, A. D. Daniels, M. C. Strain, O. Farkas, D. K. Malick, A. D. Rabuck, K. Raghavachari, J. B. Foresman, J. V. Ortiz, Q. Cui, A. G. Baboul, S. Clifford, J. Cioslowski, B. B. Stefanov, G. Liu, A. Liashenko, P. Piskorz, I. Komaromi, R. L. Martin, D. J. Fox, T. Keith, M. A. Al-Laham, C. Y. Peng, A. Nanayakkara, M. Challacombe, P. M. W. Gill, B. Johnson, W. Chen, M. W. Wong, C. Gonzalez, J. A. Pople, Gaussian 03, revision E.01; Gaussian, Inc., Wallingford, CT, 2004.

Table S1. Crystallographic Data for **2**·2acetone.

Formula	C ₅₀ H ₄₈ Cu ₁ F ₁₂ N ₄ O ₂ P ₂
Fw	1090.43
Lattice	Monoclinic
<i>a</i> , Å	16.8048(8)
<i>b</i> , Å	16.1422(7)
<i>c</i> , Å	18.8487(9)
β , °	99.9454(13)
<i>V</i> , Å ³	5036.2(4)
Space group	<i>P</i> 2 ₁ / <i>c</i>
<i>Z</i>	4
ρ (calc.), g cm ⁻³	1.438
<i>F</i> (000)	2236.00
μ (MoKα), cm ⁻¹	5.85
Radiation (λ), Å	0.71073
Temp., K	173
<i>R</i> ^a	0.0693
<i>R</i> _w ^b	0.1084
GOF	1.189
No. of observations	3993
No. of variables	688

^a*R* = $\Sigma ||F_o| - |F_c|| / \Sigma |F_o|$. ^b*R*_w = $[\sum w(|F_o| - |F_c|)^2 / \sum w F_o^2]^{1/2}$.

Table S2. Selected Bond Distances and Angles for **2**–**2**acetone.

Distances (Å)			
Cu(1)–O(1)	2.529(5)	Cu(1)–O(2)	2.397(5)
Cu(1)–N(1)	2.024(6)	Cu(1)–N(2)	2.020(5)
Cu(1)–N(3)	2.019(6)	Cu(1)–N(4)	2.014(5)
Angles (°)			
O(1)–Cu(1)–O(2)	178.6(2)	O(1)–Cu(1)–N(1)	89.8(2)
O(1)–Cu(1)–N(2)	90.6(2)	O(1)–Cu(1)–N(3)	88.1(2)
O(1)–Cu(1)–N(4)	90.3(2)	O(2)–Cu(1)–N(1)	90.0(2)
O(2)–Cu(1)–N(2)	90.9(2)	O(2)–Cu(1)–N(3)	92.1(2)
O(2)–Cu(1)–N(4)	88.3(2)	N(1)–Cu(1)–N(2)	91.4(2)
N(1)–Cu(1)–N(3)	177.7(2)	N(1)–Cu(1)–N(4)	89.4(2)
N(2)–Cu(1)–N(3)	89.5(2)	N(2)–Cu(1)–N(4)	178.8(2)
N(3)–Cu(1)–N(4)	89.7(2)		

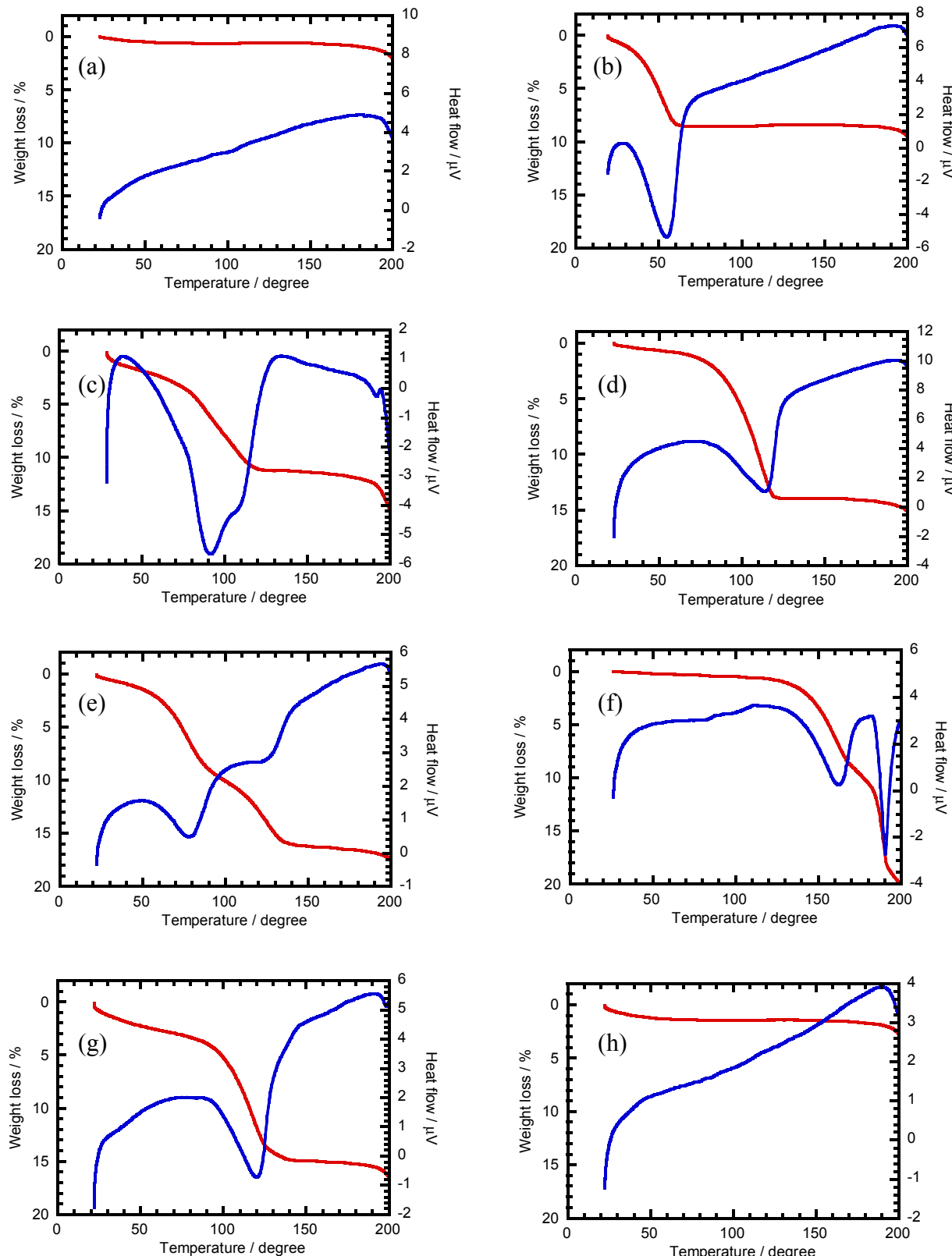


Fig. S1. TG (red) and DTA (blue) curves of (a) **1** and **1** after exposure to (b) H_2O , (c) MeCN, (d) acetone, (e) 2-butanone, (f) DMF, (g) propionitrile, and (h) THF. In the case of (b)-(g), the adsorbed amount of guests is estimated to be 3.7, 2.1, 2.0, 2.0, 2.0, and 2.2 mol per 1 mol of **1**, respectively.

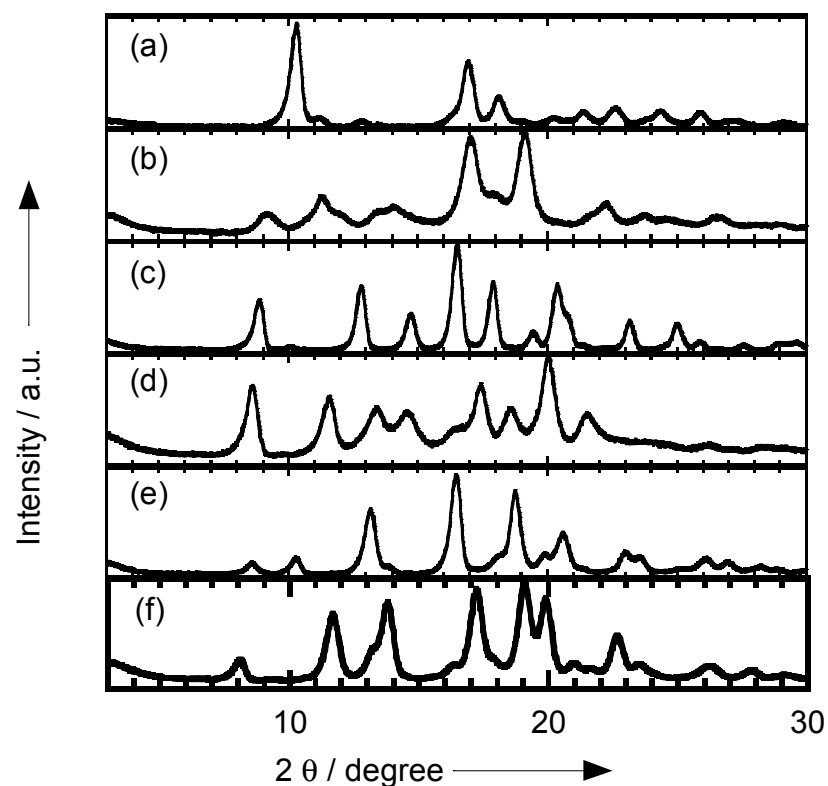


Fig. S2. XRD patterns of (a) **1** and **1** after exposure to (b) MeCN, (c) acetone, (d) 2-butanone, (e) DMF, and (f) propionitrile vapors.

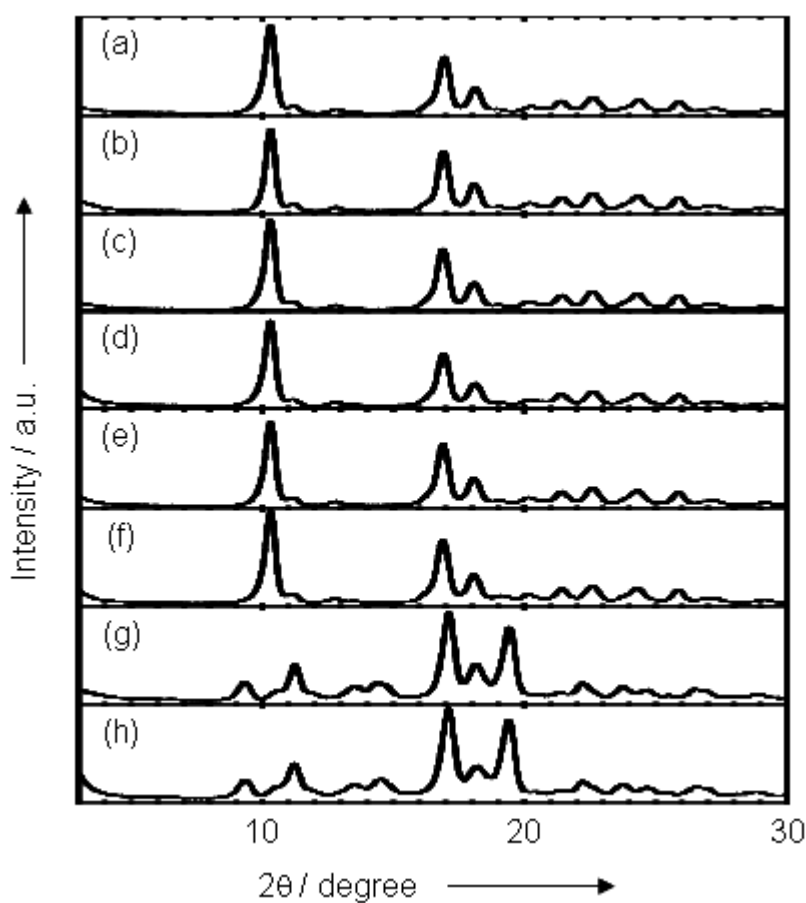


Fig. S3. XRD patterns of (a) **1** and **1** after exposure to (b) EtOH, (c) diethylether, (d) THF, (e) hexane, (f) benzene, (g) MeOH, and (h) H₂O vapors. In the case of MeOH, the observed XRD pattern is similar to (h), suggesting that the H₂O molecules existing in the atmosphere are adsorbed to **1**.

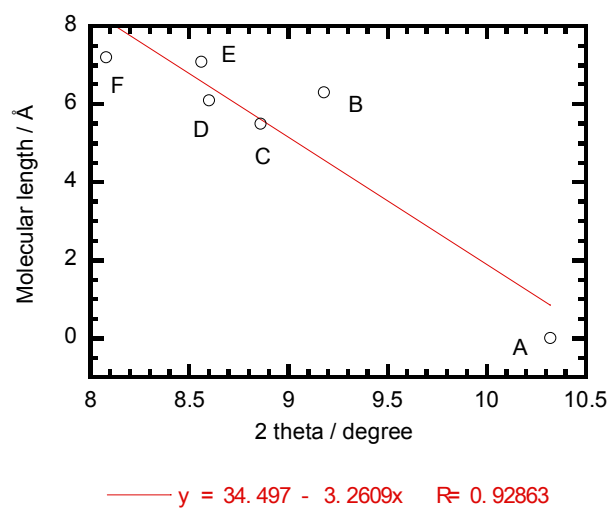


Fig. S4. Plot of molecular length of guests (A: nothing, B: MeCN, C: acetone, D: 2-butanone, E: DMF, F: propionitrile) vs. 2θ value of most low-angle XRD peak. The molecular lengths of guests are defined as shown in Fig. S5.

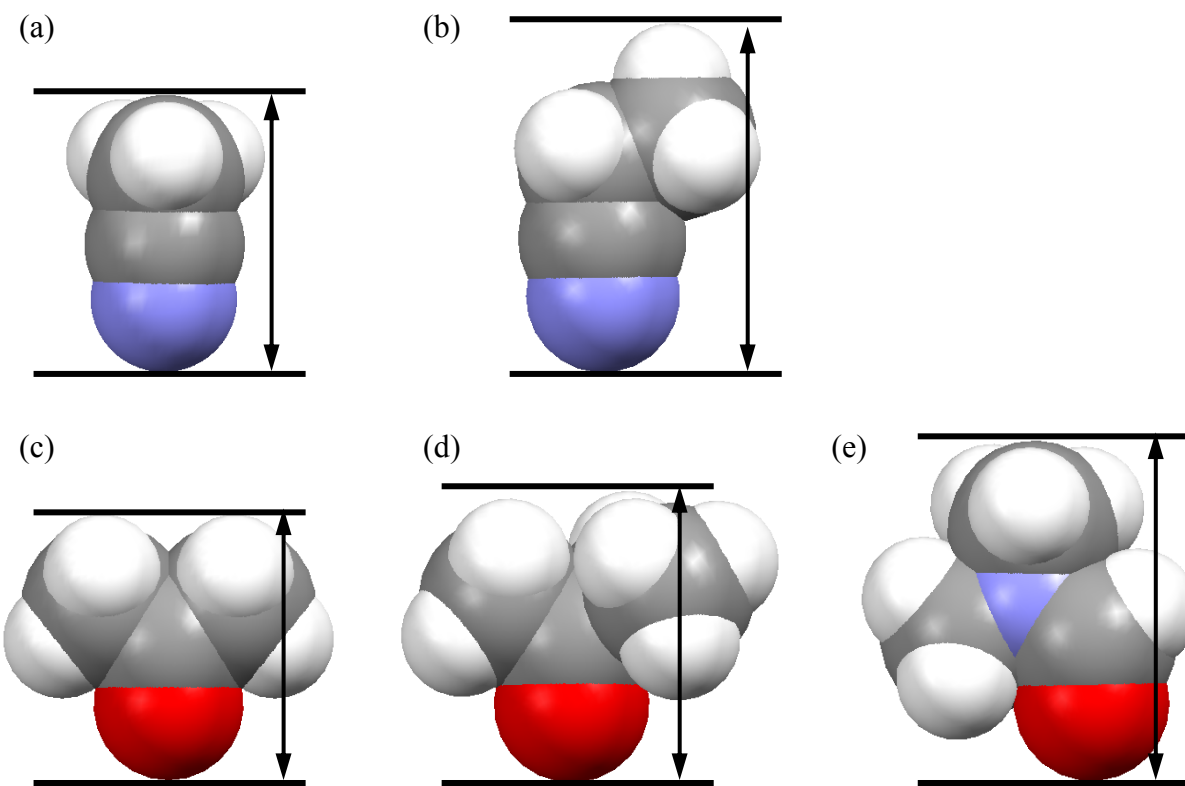


Fig. S5. The molecular lengths of guests ((a) MeCN, (b) propionitrile, (c) acetone, (d) 2-butanone, and (e) DMF). In our previous report, the angles of axial bonds, Cu-O=C (acetone) and Cu-N≡C (MeCN), were roughly 180° . The lengths of guests are calculated parallel to the C=O or C≡N axis of guests, because the sizes of guests parallel to such directions predominately affect the packing of one-dimensional chains.

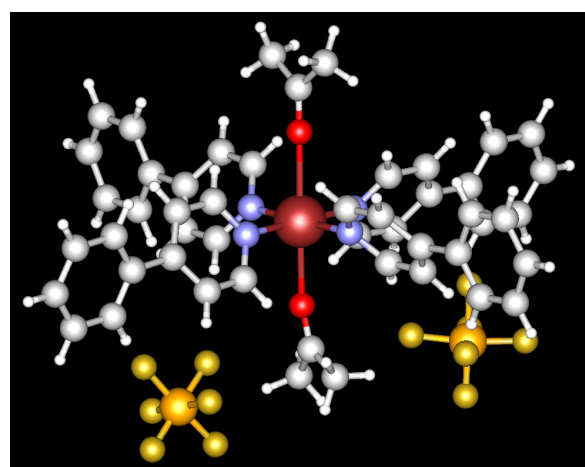


Fig. S6. Crystal structure of **2** in acetone (Cu: dark red, O: red, N: blue, C: gray, H: white, F: yellow, P: bright yellow)

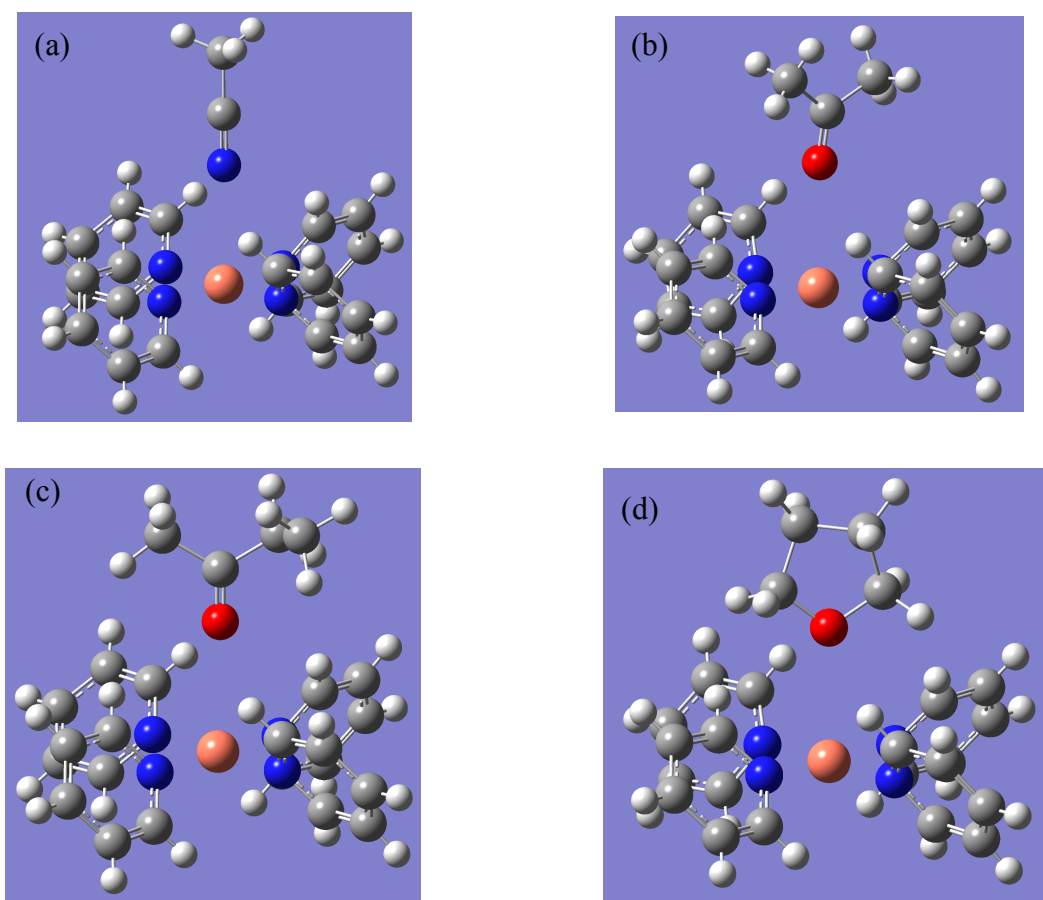


Fig. S7. The model structures of $[\text{Cu}(\text{pyridine})_4(\text{G})]$ ($\text{G} = \text{(a) MeCN, (b) acetone, (c) 2-butanone, and (d) THF}$) used in calculations.

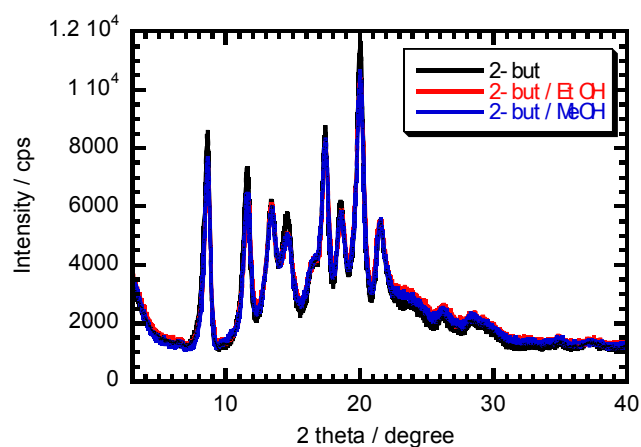


Fig. S8. XRD pattern of **1** after exposure to 2-butanone vapor for 22 hours (black), 2-butanone/EtOH (38:62) vapor for 1 hour (red), and 2-butanone/MeOH (40:60) vapor for 1 hour (blue). They show that the complete structural transformation from **1** to $\{[\text{Cu}(\text{bpetha})_2(2\text{-butanone})_2] \cdot 2\text{PF}_6\}_n$ ($\mathbf{1} \supseteq \mathbf{2}$ (2-butanone)).

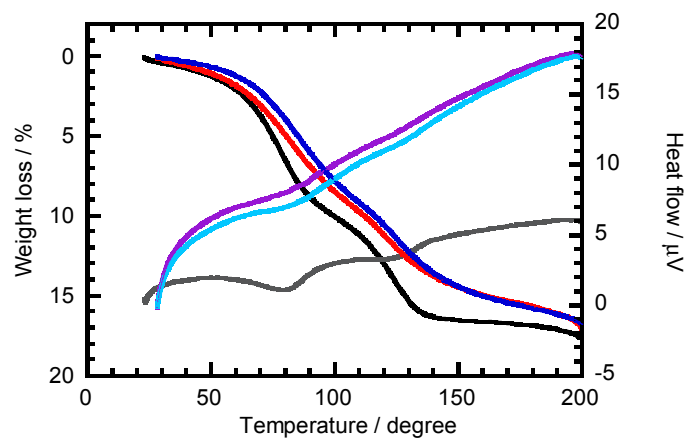


Fig. S9. TG and DTA curves of **1** after exposure to 2-butanone vapor for 22 hours (TG: black, DTA: gray), 2-butanone/EtOH (38:62) vapor for 1 hour (TG: red, DTA: purple), and 2-butanone/MeOH (40:60) vapor for 1 hour (TG: blue, DTA: sky-blue).

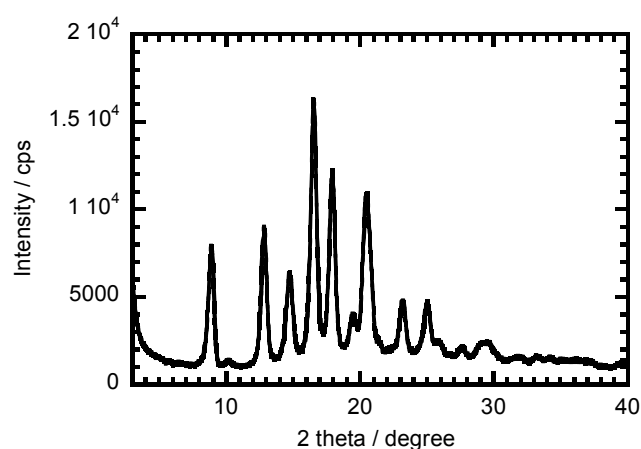


Fig. S10. XRD pattern of **1** after exposure to 2-butanone/EtOH (38:62) vapor for 1 hour and then immersion to acetone-d⁶ solution. This shows that the adsorbed guests are completely replaced by acetone-d⁶ guests.

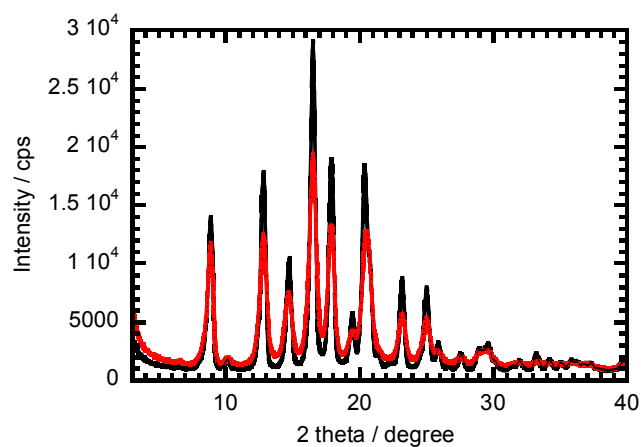


Fig. S11. XRD patterns of $\{[\text{Cu}(\text{bpetha})_2(\text{acetone})_2]\cdot 2\text{PF}_6\}_n$ (**1** \supset 2acetone, black) and $\{[\text{Cu}(\text{bpetha})_2(\text{acetone-d}^6)_2]\cdot 2\text{PF}_6\}_n$ (**1** \supset 2acetone-d⁶, red). **1** \supset 2acetone-d⁶ was prepared by exposure of **1** to acetone-d⁶ vapor.

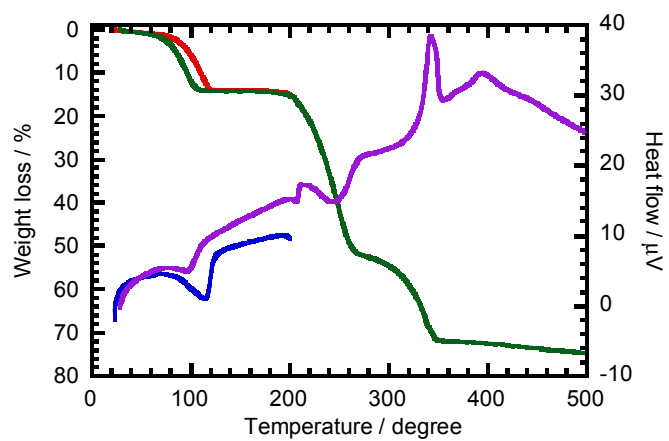


Fig. S12. TG and DTA curves of **1**-2acetone (TG: red, DTA: blue) and **1**-2acetone-d⁶ (TG: green, DTA: purple).

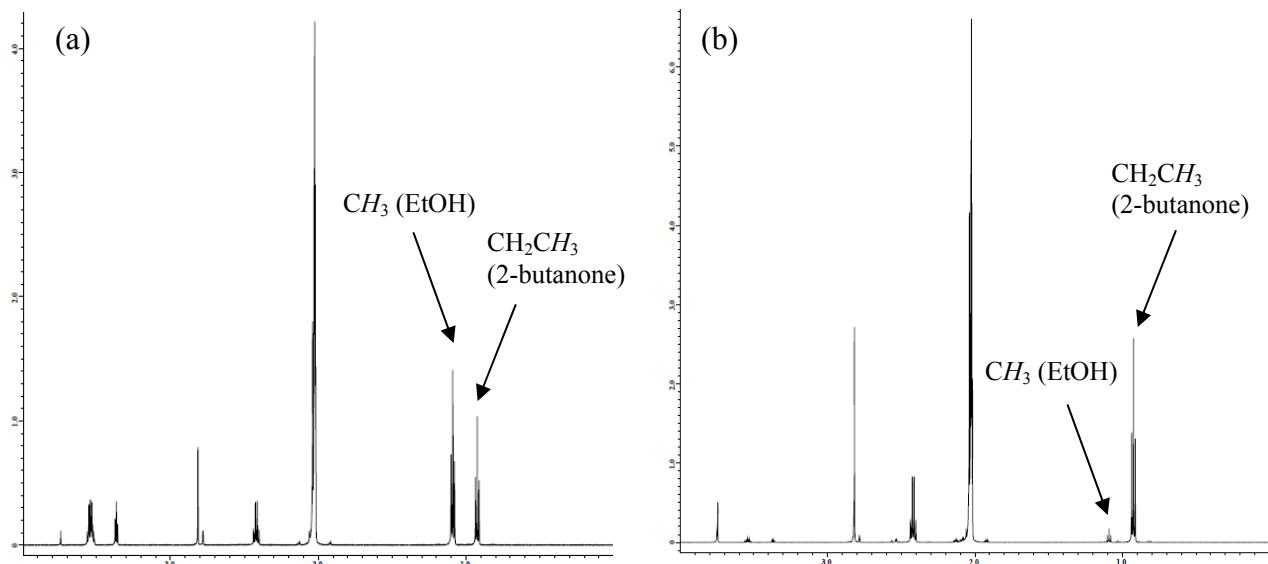


Fig. S13. ¹H-NMR spectra of (a) 38:62 mixture of 2-butanone and EtOH, and (b) guests adsorbed in **1** after exposure to mixed vapor of 2-butanone and EtOH (38:62), in acetone-d⁶ at 298 K.

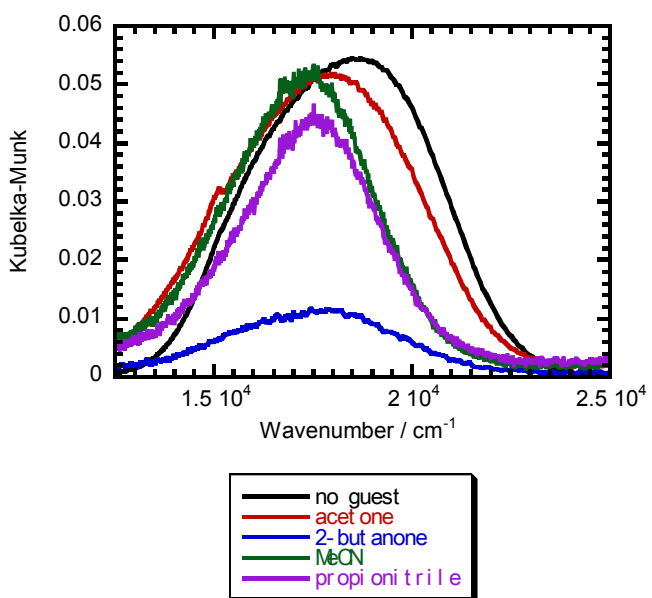


Fig. S14. The UV-vis reflection spectra of **1**, **1**•2acetone, **1**•2(2-butanone), **1**•2.1MeCN, and **1**•2.2propionitrile. In the case of Cu(II) complexes with tetragonal distortion, there are three electronic transitions, $d_{z^2} \rightarrow d_{x^2-y^2}$, $d_{xy} \rightarrow d_{x^2-y^2}$, and $d_{xz}, d_{yz} \rightarrow d_{x^2-y^2}$. The last forms the highest energy component. Hence, the absorption maxima of the spectra shift to lower frequencies as the donor ability of solvent increases. The absorption maxima of the compounds with guests (**1**•2acetone, **1**•2(2-butanone), **1**•2.1MeCN, and **1**•2.2propionitrile) were located at lower wavenumber region than **1**, indicating the weak coordination of Lewis base guests (acetone, 2-butanone, MeCN, and propionitrile). Such a spectral shift caused the change in color from purple to bluish-purple.